



## Behavior of Composite Parts Adhesively Joined with Single Lap Joint and Intermediated Material Under Tensile Load

Ismail Yasin Sülü

Inönü University, Department of Mechanical Engineering, Malatya, Turkey

✉: [ismail.sulu@inonu.edu.tr](mailto:ismail.sulu@inonu.edu.tr), : 0000-0002-2648-6294

Received: 13.05.2023, Revised: 17.07.2023, Accepted: 03.08.2023

### Abstract

*In research, composite parts adhesively joined with single-lap joint (SLJ) and intermediated material under tensile load were examined by finite element analysis (FEA). While T700 Carbon/epoxy was used for composite parts and intermediate material, DP 410 type was preferred for adhesive. The numerical studies were carried out by ANSYS 14.5 based on finite elements method. The von-Mises failure criteria and the Tsai-wu failure criteria were respectively considered for adhesive and composites. The analyses were firstly actualized to determine the failure loads for each parameter situation. The stresses at obtained failure load for each parameter state were investigated. The critical equivalent stresses on adhesive layers were examined and the critical stress lines for length and width was determined. The distributions of normal and shear stresses in all directions were obtained by considering critical stress line on adhesive layers. Similarly, the von-Mises stress distributions were obtained. Considering critical stress lines, the stress distributions on width and length of overlap dimensional were compared. The effects of overlap dimensional, orientation angle and intermediated material on effect of joint zone were investigated.*

**Keywords:** Intermediated material, finite element analysis, orientation angles, stress analysis, adhesive, joint design.

### 1. Introduction

Composite materials is preferred many industries, such as aircraft, aerospace, automotive, marine, sport equipment and various areas such as lightweight and excellent structural performance [1-3]. The use of adhesive bonding for combining structures as different from other conventional methods is created many advantages. It enables a simple and efficient joint procedure while obtaining any weight decrease and limiting material failure [4]. Also, due to easy application and good mechanical properties of adhesives, there is also an increasing demand for adhesives for repairing and joining damaged parts [5].

Adhesive applications are widely used to be joined many materials. Important factors in bonding processes are the working life and strength of the joined area. Therefore, many researches about joint design are carried out. Single-lap joint (SLJ) joining techniques are also used in composite-metal connections in different loading situations. When the effect of the adhesive to different types of materials cannot be similar, it will show different mechanical behavior as a result of combining different materials [6-8]. Moreover, different studies on SLJ are available in the literature. Shang and et al. [9] fabricated and tested SLJs with a hard and brittle adhesive. It was shown that SLJs joined with the tough adhesive failed by interlaminar delamination in the CFRP, SLJs bonded with the brittle adhesive failed cohesively in the adhesive. In a study on joint lifetimes, tensile tests were actualized on the SLJs to define the highest loads for fatigue tests and also to evaluate their quasi-static behaviors. They determined fatigue loads according to the test results and conducted studies at different adherents thicknesses. Also, they determined the fatigue



loads according to the test results and conducted studies on the strength of SLJs with different adherents thicknesses [10].

Moreover, Huang and et al. [11] investigated the influence of temperature, impact energy and stiffness combination on residual tensile properties. It was noted that both temperature and impact energy now have a strong correlation with the static properties, and decreasing the relative stiffness ratio can decrease the residual tensile strength of SLJs. In another study, Shi and et al. [12] carried out numerical studies and experimental on the FT durability of basalt FRP (BFRP) SLJs. It was noted that the tensile properties of different BFRPs were not affected by FT cycling, while significant deterioration was seen for the bonding behavior of the epoxy resin and fiber-matrix interface. Choudhury and Debnath [13] have experimentally examined mechanical characterization of adhesively joined SLJ of green composites under tensile and compressive loads. They found that increasing the overlap length dimensions positively affects the mechanical performance. Moreover, there were studies on the joining of different materials using the single-lap joint method and the mechanical performance of the joint area. In most studies, parameters such as different overlap sizes, adhesive thickness, different loadings, adhesive type and orientation angle of composites have been taken into account [13-20].

In this investigative, composite plates adhesively joined with SLJ and intermediated materials were investigated by non-linear FEA. In this joint design, composite layer between adhesive layers were put into. Failure loads were obtained for parameters such as over-lap dimensional and orientation angles. Due to be important the adhesive zone, shear stresses, stresses at all directions and the equivalent stress on adhesive layers were determined at the time of the failure. The aim of the research is to demonstrate that the adhesive is easy to use, high strength and more practical in composite plates for the industry.

## 2. 3-D Finite Element Modeling

Composite plates bonded with intermediated material under tensile load were presented in Fig. 1. Composite adherends were eight layered, intermediated material was one layered composite. Composites and adhesive were considered carbon/epoxy (T700) and DP 410 respectively. The material constants of adhesive in Table 1 and composites Table 2 were presented. The parameters in Table 3 were considered for orientation angles. The  $\sigma$ - $\epsilon$  behavior of adhesive was shown in Fig. 2.

The each layer thickness and the thickness of intermediated composite material were 0.2 mm ( $t$ ), the total thickness of composite plates was  $8 \times t$ , and the thickness of adhesive layer was 0.2 mm ( $t_1$ ). The lengths ( $L$ ) of the composite parts were 62.5 mm, the over-lap lengths ( $L_1$ ) and widths were 15 mm, 20 mm, 25 mm. Orientation angle of intermediated composite material was considered Type I for all joints.

Table 1. Material properties for DP 410 adhesive [18-22]

Properties	DP 410
Young's modulus $E_a$ (MPa)	2567.45
Poisson's ratio $\nu_e$	0.31
Yield strength $\sigma_y$ (MPa)	38
Ultimate tensile strength $\sigma_t$ (MPa)	40.79
Ultimate tensile strain $\epsilon_t$ (mm·mm <sup>-1</sup> )	0.027

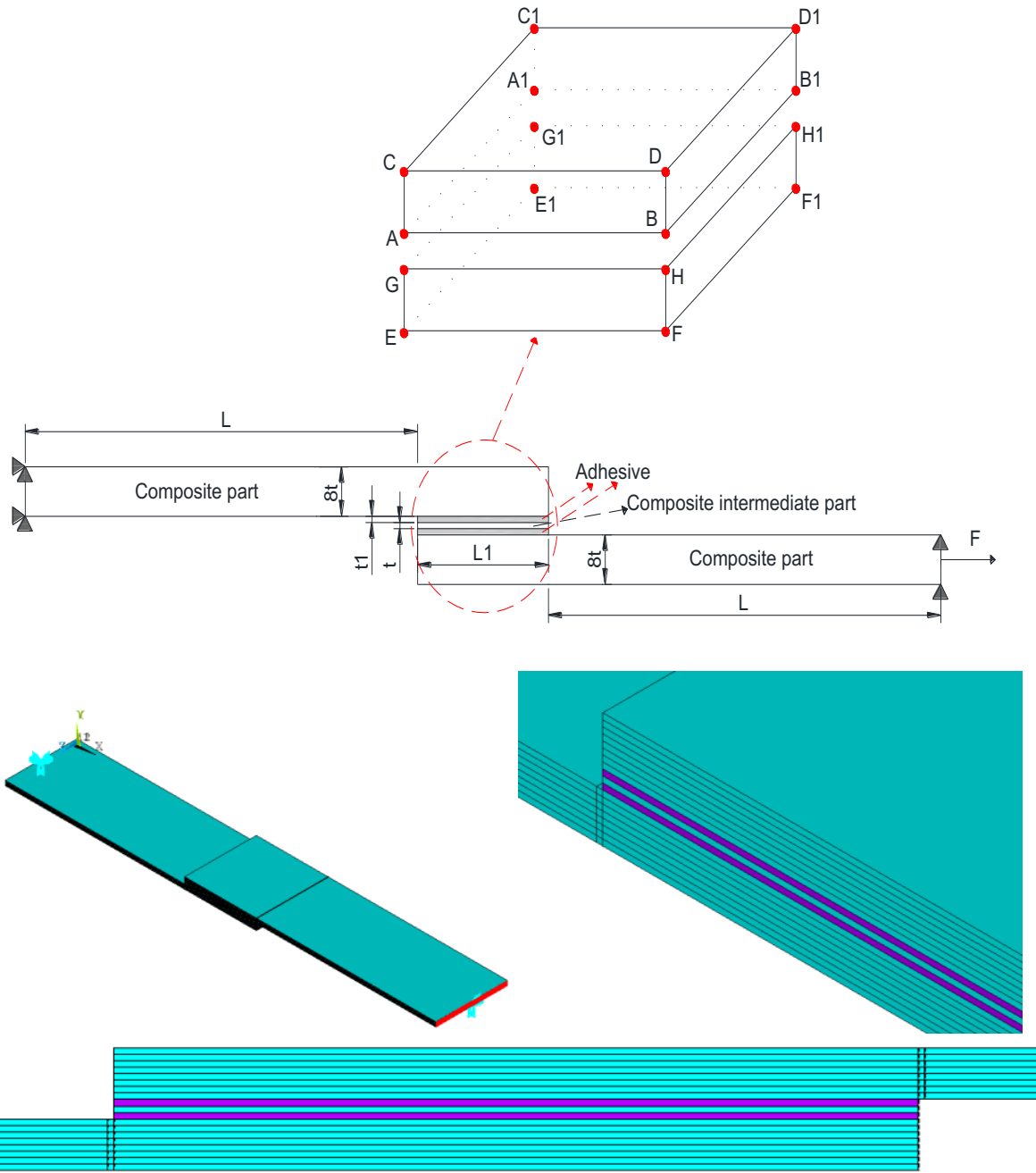


Fig. 1. Composite plates joined with SLJ and intermediated material

In the non-linear FEM, composite plates bonded with SLJ and intermediated materials were simulated via FEM. 3D-FEM was generated during the analysis of joint with SLJ and intermediated materials. In the model, SOLID186 was considered in the macro ANSYS 14.5 version generated. Its properties were 20 node isoperimetric quadrangular elements and three degrees of freedom for each node in all directions. One end of plates jointed was fixed nodal in all directions, other one was fixed in y and z directions. In Fig. 3, the joint design configuration, detailed mesh status and boundary conditions considered in research were presented. Failure analyses were realized for joints with SLJ and intermediated materials. The von-Mises failure criteria and Tsai-wu failure criteria were respectively considered for the adhesive and the composite [18-22].

Table 2. Material properties for T700 [23]

Properties	Carbon/epoxy (T700)
$E_x$ (MPa)	132000
$E_y$ (MPa)	10300
$E_z$ (MPa)	10300
$G_{xy}$ (MPa)	6500
$G_{yz}$ (MPa)	3910
$G_{xz}$ (MPa)	6500
$\nu_{xy}$	0.25
$\nu_{yz}$	0.38
$\nu_{xz}$	0.25
$T_x$ (MPa)	2100
$T_y$ (MPa)	24
$T_z$ (MPa)	24
$C_x$ (MPa)	1050
$C_y$ (MPa)	132
$C_z$ (MPa)	132
$S_{xy}$ (MPa)	75
$S_{yz}$ (MPa)	75
$S_{xz}$ (MPa)	75

Table 3. Angle parameters

Orientation angles( $^{\circ}$ )	
[0/ 0/ 0/ 0/ 0/ 0/ 0/ 0]	Type I
[15/ -15/ 15/ -15/ 15/ -15/ 15/ -15]	Type II
[30/ -30/ 30/ -30/ 30/ -30/ 30/ -30]	Type III
[45/ -45/ 45/ -45/ 45/ -45/ 45/ -45]	Type IV
[60/ -60/ 60/ -60/ 60/ -60/ 60/ -60]	Type V
[75/ -75/ 75/ -75/ 75/ -75/ 75/ -75]	Type VI
[90/ 90/ 90/ 90/ 90/ 90/ 90/ 90]	Type VII

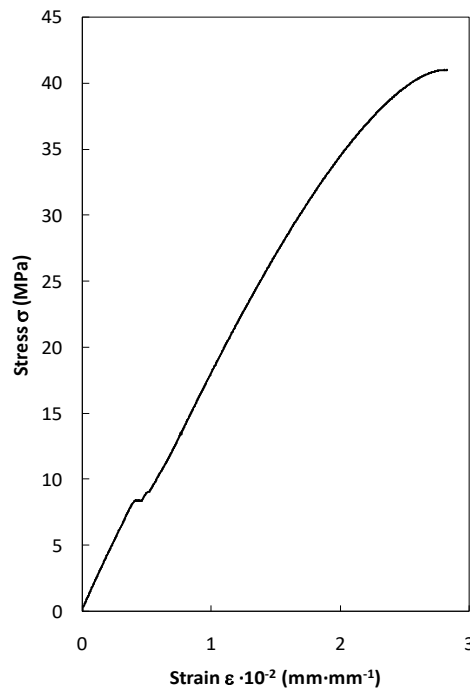


Fig. 2. Tensile stress–strain curve of DP 410 [18-22]

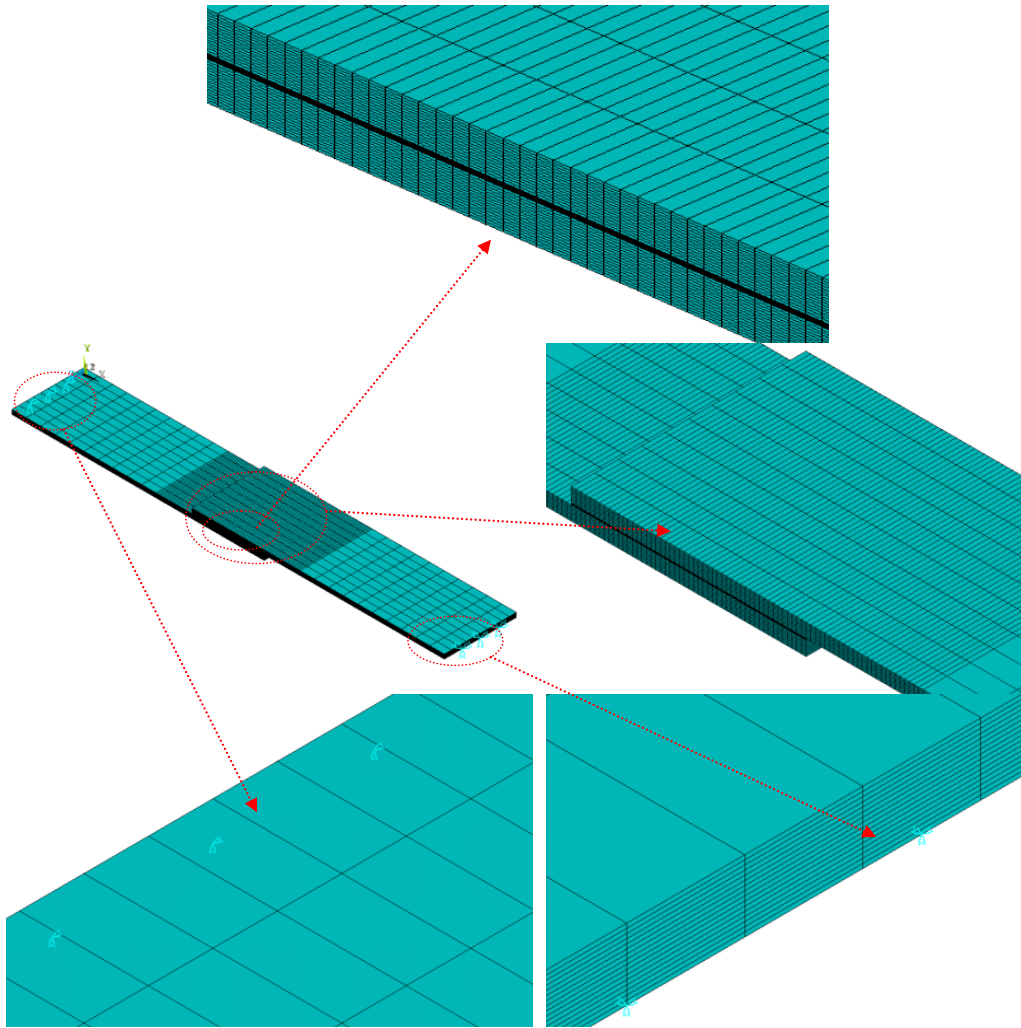


Fig. 3. Detailed mesh structure and boundary conditions on the model

### 3. Results and Discussion

#### 3.1. Influence on stress distributions of L1 lengths and angles

Stress distributions of joint with SLJ and intermediate material were researched, the analysis was realized considering the dimensional and all orientation angles parameters of the 20 mm strap joint. Failure always created on composite parts, but the strength of the adhesion surfaces of the adhesive is important in bonding processes. Therefore, bond-lines on the adhesive in the joint region (Fig. 1) were considered. In order the determination of critical lines on joint region,  $\sigma_{\text{eqv}}$  distributions of the all lines on adhesive layers were checked. The  $\sigma_{\text{eqv}}$  on C-D and D-D1 were presented both maximum in Fig. 4a and Fig. 4b. So, the stresses were investigated for the C-D line on edges and the D-D1 line on width.

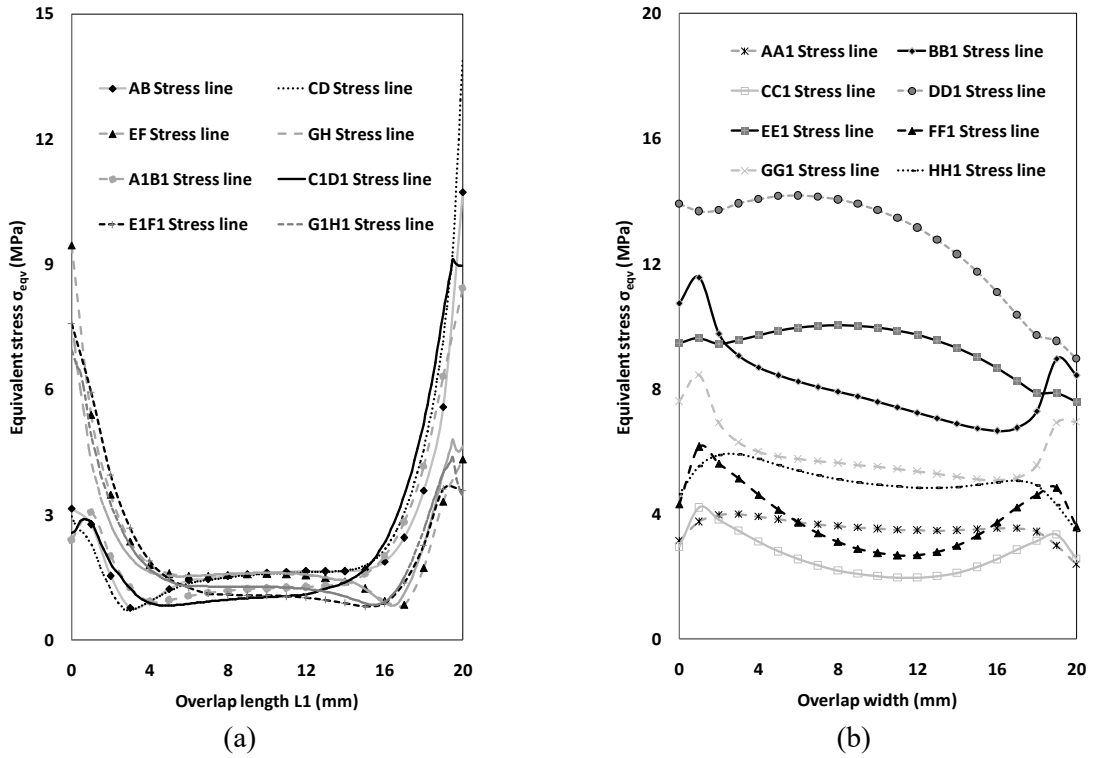


Fig. 4. Comparison the equivalent stresses throughout all lines (Fig. 1) for 20 mm of  $L_1$  and Type IV, a) On edges, b) On width

The stress behaviors of the joints with intermediated material and SLJ were given in Figs. 5 to 6. The stresses on critical lines of joint were generally maximum at the C-D on edge and the D-D1 on width. This was because the composite part on which the loading was made and the C-D and D-D1 lines on the adhesive were directly exposed to the damage load.

Due to be critical area adhesive layers, the distributions of  $\sigma_x$ ,  $\sigma_y$ ,  $\sigma_z$ ,  $\sigma_{xy}$ ,  $\sigma_{xz}$ ,  $\sigma_{yz}$  and  $\sigma_{eqv}$  on adhesive were determined at damage loads. When Figs. 5 to 6 were investigated, the stresses were shown that were determined on critical lines as a result of joints with SLJ and intermediated material.

In Figs. 5 to 6, the actions of angles on the adhesive layers were presented. It could be said that  $\sigma_x$ ,  $\sigma_y$ ,  $\sigma_z$ ,  $\sigma_{xy}$  and  $\sigma_{eqv}$  on critical line was the highest when composite parts with Type VII were used.  $\sigma_{yz}$  was the highest when joints with Type V were used. The  $\sigma_{xz}$  was the highest when joints with Type VI orientation angles were considered.

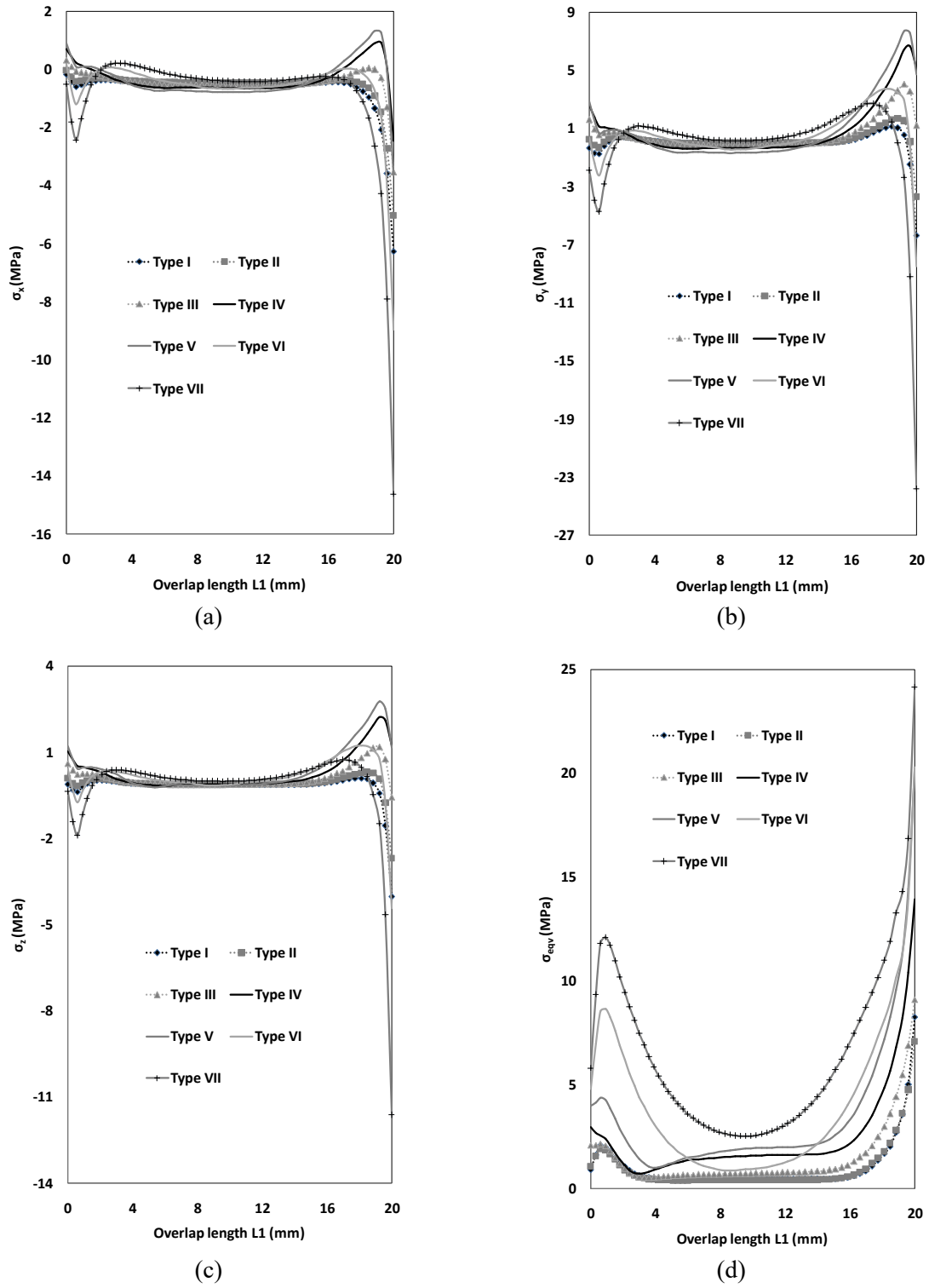


Fig. 5. Comparison of stresses for all orientations throughout C-D for 20 mm of  $L_1$ , a) In x-direction, b) In y-direction, c) In z-direction, d) Equivalent stress  $\sigma_{eqv}$

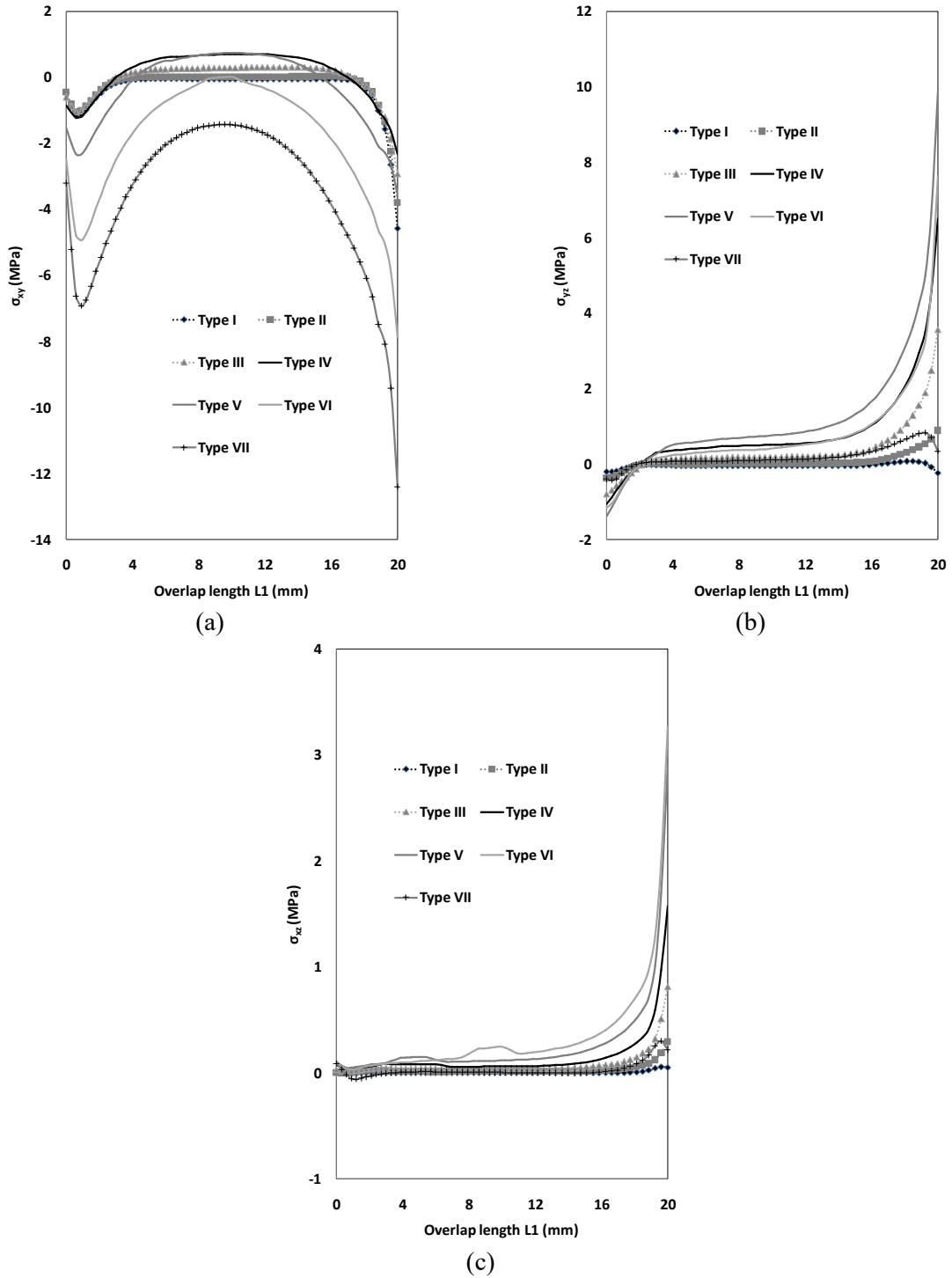


Fig. 6. Comparison of shear stresses for all orientations throughout C-D for 20 mm of  $L_1$ , a)  $\sigma_{xy}$ , b)  $\sigma_{yz}$ , c)  $\sigma_{xz}$

The  $\sigma_{eqv}$  stresses on C-D and D-D1 were examined in Fig. 7. Stress values in C-D and D-D1 stress lines for each orientation angles were compared together on the same graphs. While there was a regular stress distribution in the C-D and D-D1 stress lines at the Type I, Type II and Type VII orientation angles, it was observed that there was no regular stress distribution at the other orientation angles. It was seen that the maximum values were reached in the middle sections, while it was minimum in the ends of overlap. But this situation seems to be different in Type III, Type IV, Type V and Type VI. Specially, effect of Type IV angle was more different. It could be stated that the angles are influential both across the edge and width in the overlap region.



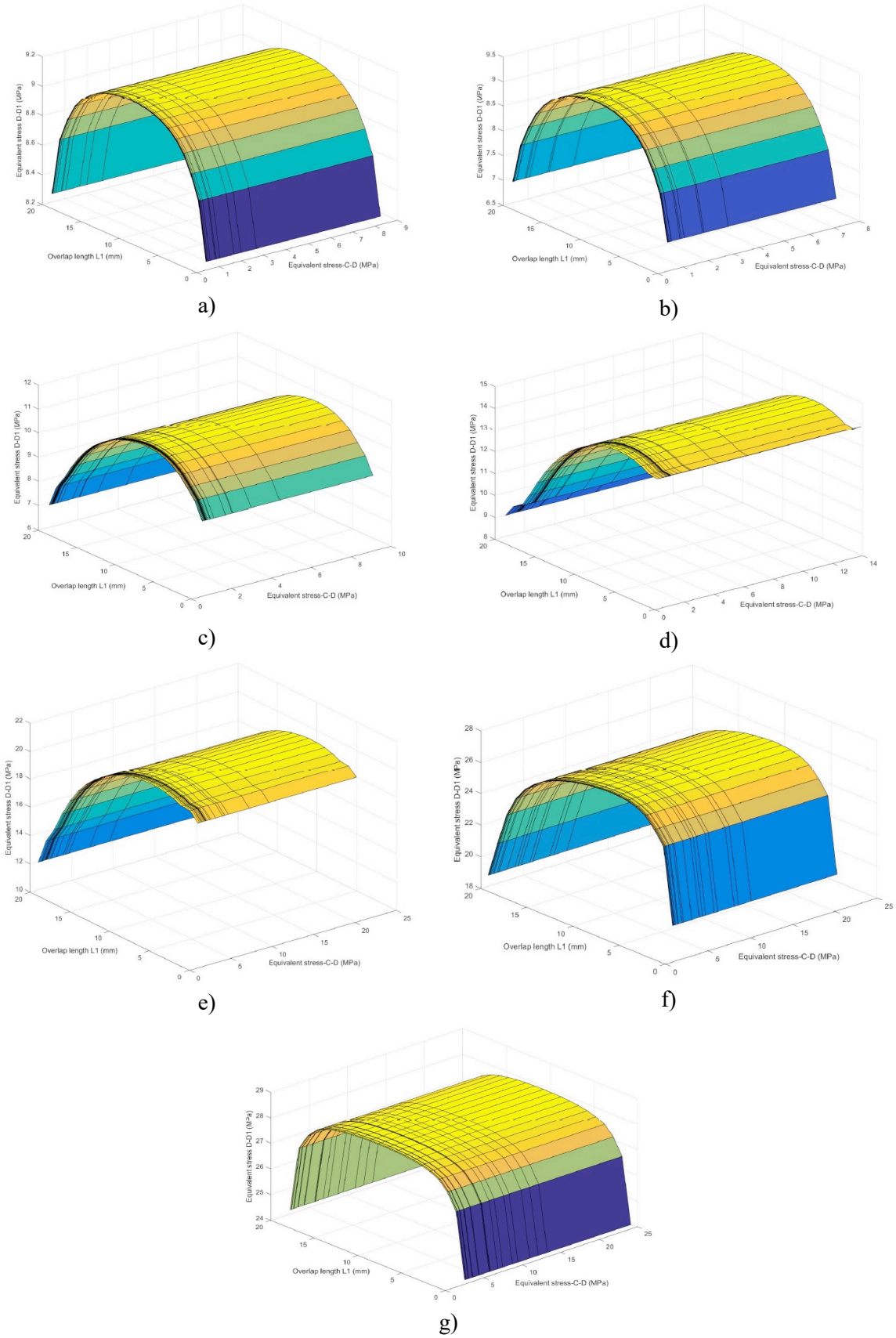


Fig. 7. The equivalent stresses compared throughout C-D and D-D1 for 20 mm on adhesive layer, a) Type I, b) Type II, c) Type III, d) Type IV, e) Type V, f) Type VI, g) Type VII

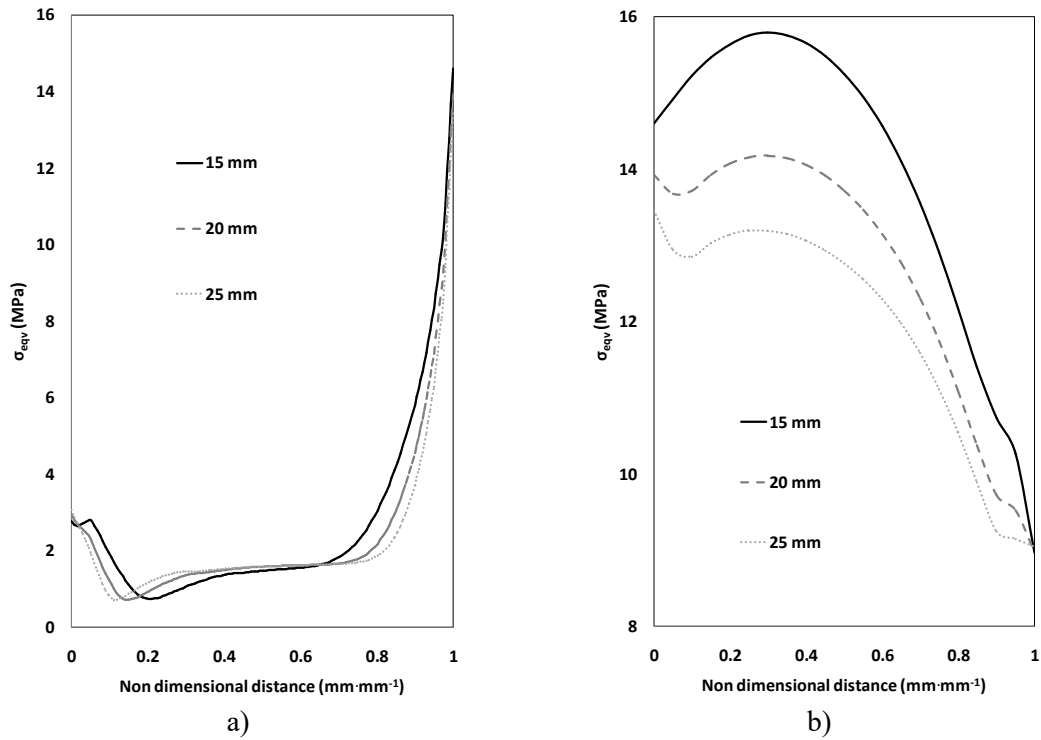


Fig. 8. Comparison the equivalent stresses for different line length (Fig. 1) considering Type IV, a) On edges, b) On width

In Figs. 8a and 8b,  $\sigma_{eqv}$  distributions on adhesive layer were investigated for all overlap dimensional with Type IV. On the edge, it could be stated that  $\sigma_{eqv}$  stresses distribution for all L1 lengths was very close. Otherwise,  $\sigma_{eqv}$  distributions for all overlap on width were different.  $\sigma_{eqv}$  distributions over the widths were listed from maximum to minimum as 15 mm, 20 mm and 25 mm, respectively. As a result, it could be said that different  $\sigma_{eqv}$  distributions were observed at different width lengths. Therefore, it could be said that overlap  $\sigma$  dimensional was important for joining.

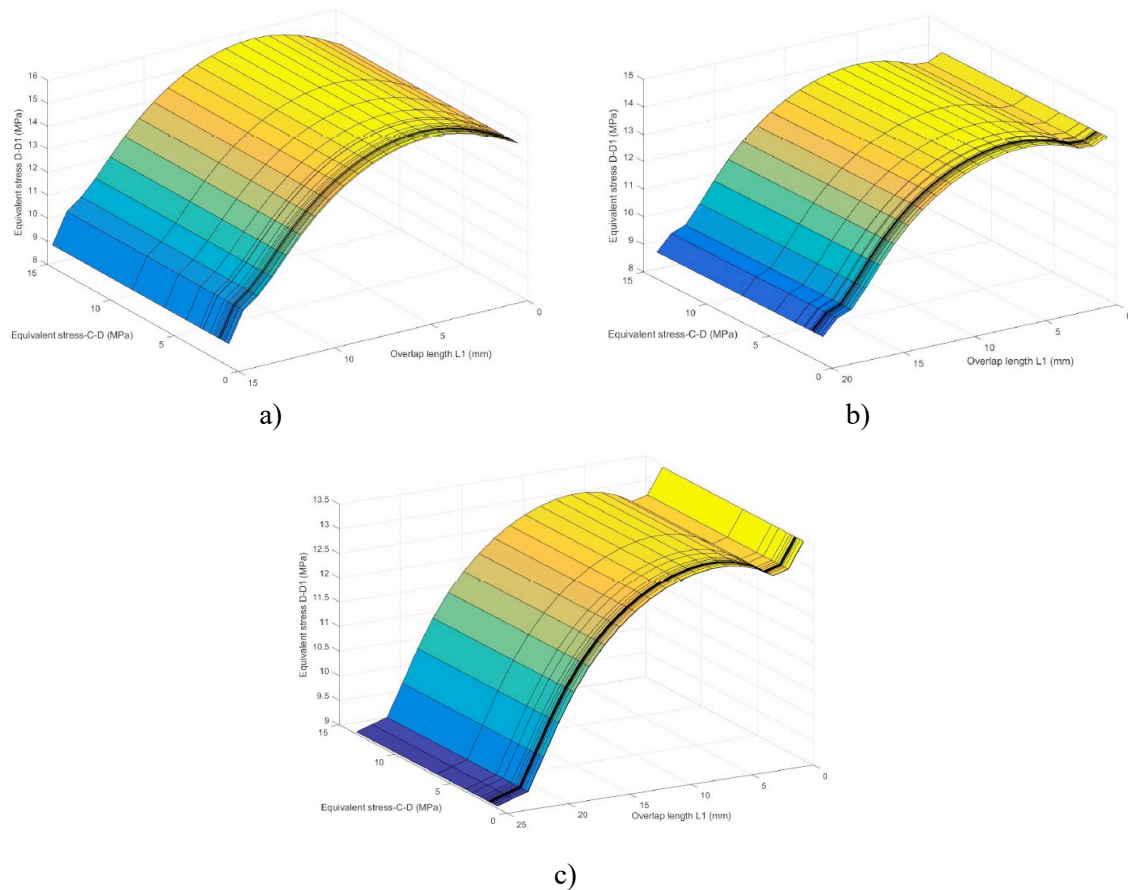


Fig. 9. Comparison the equivalent stresses for C-D and D-D1 considering Type IV, a) for 15 mm, b) for 20 mm, c) for 25 mm

As shown in Fig. 9, the equivalent stresses on C-D and D-D1 were investigated for different overlap dimensional and Type IV orientation angle. Stress values in C-D and D-D1 stress lines for each overlap dimensional were compared together on the single graph. It could be said that as the overlap length increases, differences in stress distributions occur. The greatest change was observed at 25 mm overlap dimensional.

### 3.2. Actions on failure load of L1 length and angles

The damage conditions of composites adhesively bonded with intermediated materials and SLJ for different parameters were presented Table 4. In Fig. 2,  $\sigma$ - $\epsilon$  behavior for adhesive was presented. In order to predict the damage load of the adhesive, the ultimate strain the ( $\epsilon^*$ ) in Table 1 was considered. The equivalent strain ( $\epsilon_{eqv}$ ) and the equivalent stress ( $\sigma_{eqv}$ ) were computed by the von Misses yield criterion and it was assumed that the damage occurred when  $\epsilon_{eqv}$  calculated reached the ultimate strain at any point of the adhesive layers. Also, for composites, damage control of composite parts and intermediate materials was carried out by Tsai-wu fracture criterion, taking into account the maximum strength values given in Table 2. A solution with nonlinear material behavior in the finite element analysis was reached by applying the load step by step to follow the equilibrium paths and iterating to a convergent solution with each load increase. Therefore, a pressure of  $0.4 \text{ N/mm}^2$  per  $\text{mm}^2$  area was for each load step. The remaining load was then applied in the last step [18-22, 24, 25].

Behaviors of  $\sigma_x$ ,  $\sigma_y$ ,  $\sigma_z$ ,  $\sigma_{xy}$ ,  $\sigma_{xz}$ ,  $\sigma_{yz}$  and  $\sigma_{eqv}$  were generated considering tensile failure load on critical stress lines. The stresses in the interfaces of joint area were shown in Figs. 4a and 4b, the

biggest stresses on the bond-lines occur for C-D and D-D1. For that reason, stresses on these lines were investigated during the research.

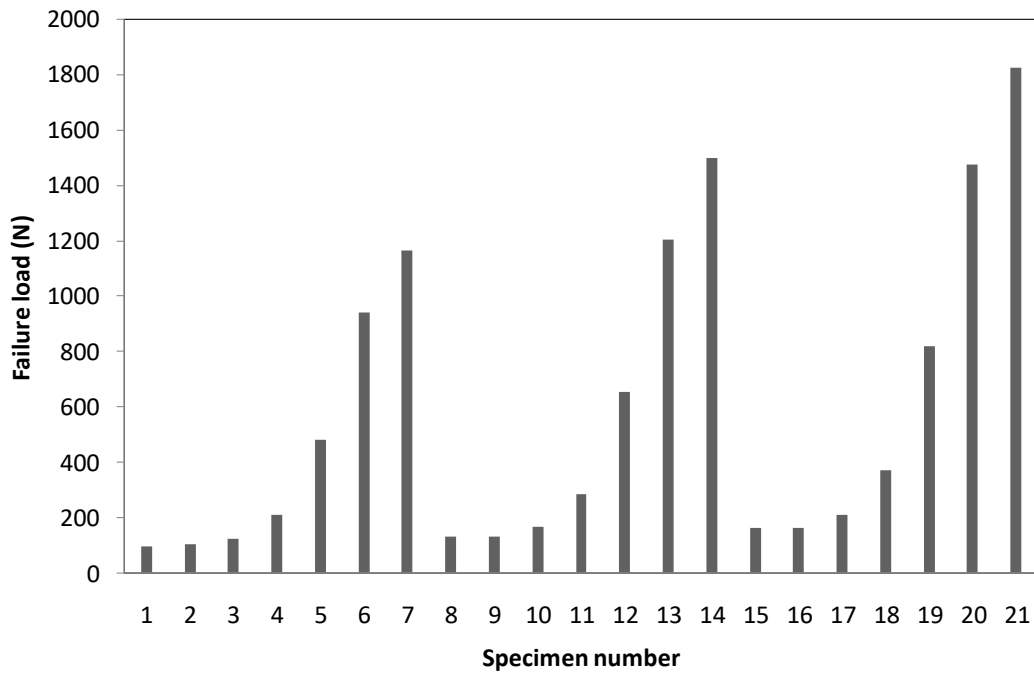


Fig. 10. The failure loads compared for all parameters

Table 4. The numerical results for joint

Specimen number	L1 (mm)	Orientation angle (°)	Failure load (N)
1	15	Type I	96.0
2		Type II	100.8
3		Type III	120.0
4		Type IV	206.4
5		Type V	480.0
6		Type VI	940.8
7		Type VII	1161.6
8	20	Type I	128.0
9		Type II	128.0
10		Type III	166.4
11		Type IV	281.6
12		Type V	652.8
13		Type VI	1203.2
14		Type VII	1497.6
15	25	Type I	160.0
16		Type II	160.0
17		Type III	208.0
18		Type IV	368.0
19		Type V	816.0
20		Type VI	1472.0
21		Type VII	1824.0

As presented in Fig. 10 and Table 4, the failure load of the joint with 25 mm L1 length and Type VII orientation angle were bigger than other. Also, the minimum predicted damage loads of joining with SLJ and intermediated material were Type I, Type II orientation angles. Moreover, the highest failure loads of the joint with SLJ and intermediated material were Type VII for all overlap lengths.

For 15 mm, 20 mm and 25 mm overlap dimensional; effects of angles were seen to be different in Table 4. Because failure regions were on composite part for all parameters and joint dimensional was different for each overlap length. Consequently, the highest damage loads were obtained in Type VII orientation angles, the smallest damage loads were obtained in Type I. Moreover, the largest damage load was obtained, since the joint area with 25 mm for L1 had the widest bond surface.

#### **4. Conclusions**

In the research, composite jointed with intermediated material were researched by FEM. The conclusions were as follows:

- The C-D on edges and the D-D1 on width were considered as critical stress lines for joint with SLJ and intermediated material.
- For joint with SLJ and intermediated material,  $\sigma_x$ ,  $\sigma_y$ ,  $\sigma_z$ ,  $\sigma_{xy}$  and  $\sigma_{eqv}$  on critical line of adhesive layer was the highest at Type VII orientation angle.
- The  $\sigma_{yz}$  was the highest on critical line of adhesive layer was the highest at Type V orientation angle.
- The  $\sigma_{xz}$  was the highest on critical line of adhesive layer was the highest at Type VI orientation angle.
- When the stresses on C-D and D-D1 were compared together, the highest stress values occurred in Type VII.
- On the edge, the equivalent stresses for all L1 lengths were very similar.
- The equivalent stresses on width were maximum for 15 mm.
- When C-D and D-D1 stress lines were compared together for all overlap dimensional, the highest stress values occurred in 25 mm dimensional.
- The failure load of the joint with 25 mm L1 length and Type VII orientation angle were bigger than other.
- The highest failure loads were joint with Type VII for all overlap lengths.
- The smallest damage loads were obtained in Type I orientation angle.

#### **References**

- [1] Xia, M., Takayanagi, H., Kemmochi, K., Analysis of multi-layered filament-wound composite pipes under internal pressure. *Composite Structures*,53, 483-491, 2001.

- [2] Sulu, Ismail Yasin , Semsettin, Temiz, Failure and stress analysis of internal pressurized composite pipes joined with sleeves.*Journal Adhesion Science and Technology*, 32 (8), 816-832, 2018.
- [3] Quan, Dong, Alderliesten, René, Dransfeld, Clemens, Tsakoniatis, Ioannis, Benedictus, Rinze, Co-cure joining of epoxy composites with rapidly UV-irradiated PEEK and PPS composites to achieve high structural integrity.*Composite Structures*, 251, 112595, 2020
- [4] Nguyen, Tuan Hung, Grogneç, Philippe Le, Analytical and numerical simplified modeling of a single-lap joint.*International Journal of Adhesion and Adhesives*, 108, 102827, 2021.
- [5] Sulu, Ismail Yasin , Temiz, Semsettin, Mechanical characterization of composite pipe systems joined using different radii pipes subject to internal pressure.*Mechanics Based Design of Structures and Machines*, 51(1), 566-582, 2023.
- [6] Sun, Guangyong, Wei, Yang, Huo, Xintao, Luo, Quantian, Li, Qing, On quasi-static large deflection of single lap joints under transverse loading.*Thin-Walled Structures*, 170, 108572, 2022.
- [7] Ma, Guoliang, Wu, Jiayu, Yuan, Hong, Interfacial shear stress analysis in single-lap adhesive joints with similar and dissimilar adherends under dynamic loading.*International Journal of Adhesion and Adhesives*, 111, 102953, 2021.
- [8] Zou, Tianchun, Fu, Ji, Qin, Jiayu, Li, Longhui, Liu, Zhihao, Failure analysis of composite-to-titanium single lap adhesive joints subjected to tensile loading.*Engineering Failure Analysis*, 129, 105734, 2021.
- [9] Shang, X., Marques, E. A. S., Carbas, R. J. C., Barbosa, A. Q., Jiang, D., da Silva, L. F. M., D., Chen, Ju, S., Fracture mechanism of adhesive single-lap joints with composite adherends under quasi-static tension.*Composite Structures*, 251, 112639, 2020.
- [10] Sahin, Resul , Akpınar, Salih, The effects of adherend thickness on the fatigue strength of adhesively bonded single-lap joints.*International Journal of Adhesion and Adhesives*, 107, 102845, 2021.
- [11] Huang, Wei, Sun, Lingyu, Liu, Yang, Chu, Yantao, Wang, Jinxi, Effects of low-energy impact at different temperatures on residual properties of adhesively bonded single-lap joints with composites substrates.*Composite Structures*, 267, 113860, 2021.
- [12] Shi, Jia-Wei, Cao, Wen-Hai, Chen, Lei, Li, Ang-Lin, Durability of wet lay-up BFRP single-lap joints subjected to freeze–thaw cycling.*Construction and Building Materials*, 238, 117664, 2020.
- [13] Lee, H. K., Pyo, S. H., Kim, B. R., On joint strengths, peel stresses and failure modes in adhesively bonded double-strap and supported single-lap GFRP joints.*Composite Structures*, 87, 44–54, 2009.
- [14] Akhavan-Safar, A., Ayatollahi, M. R., da Silva, L. F. M., Strength prediction of adhesively bonded single lap joints with different bondline thicknesses: A critical longitudinal strain approach.*International Journal of Solids and Structures*, 109, 189–198, 2017.

- [15] Abdi, H., Papadopoulos, J., Nayeb-Hashemi, H., Vaziri, A., Enhanced elastic-foundation analysis of balanced single lap adhesive joints. *International Journal of Adhesion & Adhesives*, 72, 80 – 91, 2017.
- [16] Stein, N., Mardani, H., Becker, W., An efficient analysis model for functionally graded adhesive single lap joints. *International Journal of Adhesion & Adhesives*, 70, 117 – 125, 2016.
- [17] Guin, W. E., Wang, J., Theoretical model of adhesively bonded single lap joints with functionally graded adherents. *Engineering Structures*, 124, 316 – 332, 2016.
- [18] Sülü, İsmail Yasin, Mechanical behavior of single-lap and double-lap adhesive joined composite parts. *Materials Testing*, 59(11-12), 1019-1026, 2017.
- [19] Sülü, İsmail Yasin, Mechanical testing and analysis of composite parts adhesively joined under tensile load. *Materials Testing*, 59(5), 459-465, 2017.
- [20] Sülü, İsmail Yasin, Temiz, Şemsettin, Mechanical behavior of composite parts joined through different processes. *Materials Testing*, 63, 411-419, 2021.
- [21] Sülü, İsmail Yasin, Mechanical behavior of internal pressurized composite pipes jointed with embedded tubular sleeves. *Materials Testing*, 59(3), 272-277, 2017.
- [22] Sulu, İ. Y., Temiz, Ş., Aydın, M. D., Layer effects of multi-layered face to face adhesively bonded composite pipes subjected to internal pressure. *Academic Journal of Science*, 04(3), 195-202, 2015.
- [23] Wang, B., Xiong, J., Wang, X., Ma, L., Zhang, G. Q., Wu, L. Z., Feng, J. C., Energy absorption efficiency of carbon fiber reinforced polymer laminates under high velocity impact. *Materials and Design*, 50, 140–148, 2013.
- [24] Salih, A., Aydın, M. D., 3-D non-linear stress analysis on the adhesively bonded composite joint under bending moment. *International Journal of Mechanical Sciences*, 81, 149-157, 2014.
- [25] Ozel, A., Yazici, B., Akpınar, S., Aydın, M. D., Temiz, Ş., A study on the strength of adhesively bonded joints with different adherends. *Composites Part B: Engineering*, 62, 167 – 174, 2014.